Proceedings of the IASS-SLTE 2014 Symposium
"Shells, Membranes and Spatial Structures: Footprints"
15 to 19 September 2014, Brasilia, Brazil
Reyolando M.L.R.F. BRASIL and Ruy M.O. PAULETTI (eds.)

Numerical simulation of burst-test of an ETFE membrane

Marianna Coelho*, Deane Roehl[a] and Kai-Uwe Bletzinger[b]

*
Departamento de Engenharia Civil
Universidade do Estado de Santa Catarina
Rua Paulo Malschitzki, s/n, 89219-710, Joinville, Santa Catarina, Brazil

[a]
Instituto Tecgraf and Departamento de Engenharia Civil
Pontifcia Universidade Catlica do Rio de janeiro
Rua Marques de So Vicente 225, 22453-900, Rio de Janeiro, Brazil

[b]
Lehrstuhl fuer Statik
Technische Universitaet Muenchen
Arcisstrasse 21, D-80333 Muenchen, Germany

Abstract

This work presents a numerical model for the simulation of the behavior of pneumatic structures made of ETFE material. The model is applied to the simulation of a Burst-test for which experimental measurements are available. In the experiment, samples of ETFE-foil were fixed in a bubble inflation test device between an aluminium plate and an aluminium ring.

Air was injected between the plate and the foil, resulting in a spherical deformed configuration. This test is modeled with finite elements and the numerical models are compared to experimental results. The elastoplastic material model with von Mises yield criteria is considered in the numerical analysis. Small strain and large strain were adopted for comparison. The results obtained with the numerical analysis with large strains are in accordance with the experimental results. On the other hand the results of the numerical analysis with small strains are valid only in the first steps of the analysis. These results reinforce the importance of considering a material model with large strains to model this type of material and suggest the use of von Mises plasticity for ETFE-foils.

Keywords: inflated membranes, membrane materials, finite element method, NURBS surfaces

1. Introduction

ETFE(Ethylene tetrafluoroethylene) is a polymer classified as a semi-crystalline thermoplastic. This type of polymer is more resistant to solvents and other chemicals than others. Ethylene tetrafluoroethylene consists of monomers of Ethylene (C_2H_4) and Tetrafluorethylene (C_2F_4). When these monomers are submitted to moderate temperature, pressure, and in presence of a catalyst, it polymerizes: In 1970 ETFE was produced for the first time by DuPONT with the name Tefzel . The features of Tefzel are described in the Properties Handbook [4]. According to Robinson-Gayle et ali. [9], ETFE was first used as roofing material in a zoo building in Burgers Zoo, Arnheim in the Netherlands in 1981. It was subsequently been used in various buildings predominantly in the United Kingdom and Germany. The low weight of ETFE is one of the most important features that motivates the use of this material in structural buildings. Moreover, it has been used more often on roofs, resulting in a lower cost for the foundation. The translucent property is advantageous, because it allows the utilization of natural light, reducing the energy consumption. Another property related to resource consumption and commented by Robinson-Gayle et ali. [9] is the anti-adhesive nature of ETFE. This property means that roofs and atria need to be cleaned less frequently reducing maintenance cost. The recycling potencial is other characteristic that is important in days of sustainability. Robinson-Gayle [9] relates that once the material is clean it can be recycled by heating it to its softening temperature. The softening temperature of ETFE is low so this is not a very costly operation, the recycled ETFE can be added into the hopper with virgin ETFE.

Moritz [7] cataloged and organized structures made with ETFE material from the first building (1980) to 2006, in they show the flexibility to create structural forms with this material.

Figure 1: Allianz Arena in Munich

Figure 2: Eden Project in the United Kingdom

2. Material modeling

Barthel et al. [1] carried out biaxial experiments with ETFE–foils and found that the results in both directions show matching mechanical behavior, in other words, the material behaves almost isotropically. Galliot and Luchsinger[5] performed tensile tests at many angles (15o , 30o, 60o and 75o) and also gave similar results. Barthel et al.[1], Galliot and Luchsinger [5] and Moritz [7] also showed that ETFE can present plastic behavior. Therefore the constitutive behavior for this isotropic material will be considered as elastoplastic. The formulation for an elastoplastic material with small and large strains will be described as follows.

2.1. Small strain elastoplasticity

The formulation used for the elastoplastic material is classic and it is presented for instance in the studies of Simo and Taylor [13], Simo and Hughes [12], and Souza Neto et al.[14]. The total strain **E** splits into a elastic strain $\mathbf{E}^e$ and a plastic strain $\mathbf{E}^p$:

$$\mathbf{E} = \mathbf{E}^e + \mathbf{E}^p \tag{1}$$

The elastic constitutive law considering linear elasticity is given by the relation:

$$\dot{\mathbf{S}} = \mathbf{D} : (\dot{\mathbf{E}} - \dot{\mathbf{E}}^p) \tag{2}$$

The yield condition is defined by equation *(f(**S**,k))*.

The flow rule and the hardening law in associative plasticity models is given respectively by:

$$\dot{\boldsymbol{E}}_{\boldsymbol{p}} = \gamma \frac{\partial f}{\partial \mathbf{S}} \tag{3}$$

$$\dot{\boldsymbol{\alpha}} = \gamma \frac{\partial f}{\partial k} \tag{4}$$

where γ is the consistency parameter, $\frac{\partial f}{\partial \mathbf{S}}$ is a function that defines the direction of plastic flow, and $\frac{\partial f}{\partial k}$ is a function that describes the hardening evolution.

In this work the von Mises yield criteria will be evaluated for its use with ETFE materials. The von Mises yield criteria suggests that yielding begins when J2, the second invariant of the deviatoric stress, reaches a critical value (k) [15].

$$f(J2) = \sqrt{J2} - k = 0 \quad \leftrightarrow \quad f(J2) = J2 - k^2 = 0 \tag{5}$$

Linear isotropic hardening is considered, for which the scalar hardening state variable is:

$$k = \sigma_y + H\alpha \tag{6}$$

where α is the amount of plastic flow.

The updating scheme for integration of the rate constitutive equations (2,3,4) subject to the yield condition 5 requires the formulation of a numerical algorithm. The implicit Euler or backward scheme is used to discretize the incremental constitutive problem.

The return mapping is the closest point projection (Simo and Hughes [12]). This return mapping considers a two-step algorithm called the elastic predictor/plastic corrector algorithm.

Finally the consistent elastoplastic tangent moduli is obtained. For more details of the computation of the consistent elastoplastic tangent moduli we refer to Simo and Hughes [12].

2.2. Large strain elastoplasticity

The deformation gradient F transforms the reference configuration into the actual configuration,

$$\mathbf{F} = \frac{\partial \mathbf{x}}{\partial \mathbf{X}} \tag{7}$$

where **x** is the position of a point in current configuration and **X** is the position of a point in the reference configuration.

The multiplicative decomposition of the deformation gradient **F** is the main hypothesis in the finite strain elasto-plasticity [6]. According to Lee and Liu [6], the combination of elastic and plastic strains, both finite, calls for a more careful study of the kinematics than the usual assumption that the total strain components are simply the sum of the elastic and plastic components, as for infinitesimal strain theory.

$$\mathbf{F} = \mathbf{F}^e \mathbf{F}^p \tag{8}$$

The Lagrangian description was used in the implementation, therefore the strain and stress tensors will be defined in this description.

The Green-Lagrange strain tensor is defined by:

$$\mathbf{E} = \frac{1}{2}\left(\mathbf{F}^T\mathbf{F} - \mathbf{I}\right) \tag{9}$$

The logarithmic strain measure is computed as:

$$\mathbf{E}_L = ln(\mathbf{U}) \tag{10}$$

where U is termed the right stretch tensor.

$$\mathbf{U} = \sqrt{\mathbf{C}} \tag{11}$$

where C is the right Cauchy-Green tensor.

The present implementation is carried out based on the works of Peri´c et al. [8] and Caminero et al. [2] that present an algorithm for the total Lagrangian formulation. Simo [11] showed that using the Kirchhoff stress tensor and the logarithmic strain tensor, the return mapping algorithm takes a format identical to the standard return mapping algorithms for the infinitesimal theory. In this work, the choice of the Kirchhoff stress and the logarithmic strain tensors allowed the direct use of the return mapping schemes developed for the infinitesimal theory. The consistent elastic moduli is obtained in spacial description as present in [3].

3. Burst test

Schiemann [10] and Galliot and Luchsinger [5] carried out experiments that consist in the inflation of an initially flat circular membrane, called burst test.

The burst test was performed with samples of ETFE–foil fixed in a bubble inflation test device between an aluminium plate and an aluminium ring. Air was injected between the aluminium plate and the foil, resulting in a spherical deformation. Tests were performed at room temperature, which corresponds to about 23ºC. The pressure in the bubble was recorded with a digital pressure sensor and the deformation of the bubble was measured with a 3D digital image correlation system.

The applicability of the material models present in section 2 for ETFE membranes will be evaluated based on experimental results. Figure 3 presents the experimental data from uniaxial and biaxial test of ETFE from works of Moritz [7], Galliot and Luchsinger [5], and DuPONT Tefzel [4] and an adjusted von Mises yield curve. This yield surface was generated considering an yield stress of 16MPa . Figure 3 shows that the von Mises criteria is a good approximation for the experimental data for the ETFE material. ETFE–foils behave as membranes, therefore the analyses will be carried out considering plane stress state.

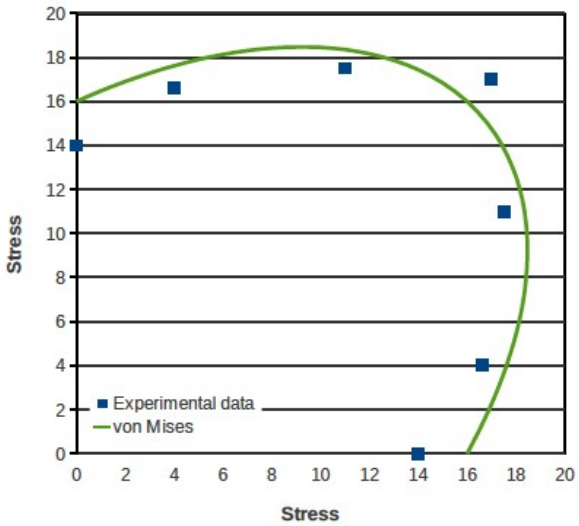

Figure 3: Experimental data from uniaxial and biaxial test of ETFE and adjusted von Mises yield curve

A finite element model is developed to compare with the results of the burst test of specimen V20 of Schiemann [10]. Figure 4 shows the mesh, geometry and boundary conditions used in the numerical model. Due to symmetry one quarter of the circular membrane is modeled.

A comparison for linear and quadratic triangular elements is carried out, in order to evaluate the results for both elements types. The mesh is composed of 800 triangular elements for both linear and quadratic element meshes with respectively 441 and 1681 nodes. Figure 5 presents the results of pressure versus displacement for both

meshes. These results are the same for the linear and quadratic, therefore seeking computation efficiency the linear triangular element is chosen to be used in the analysis to follow.

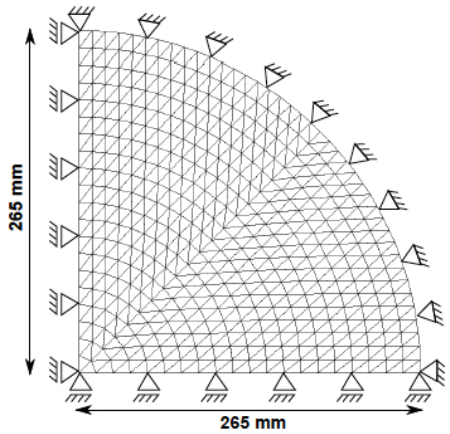

Figure 4: Geometry, mesh and boundary conditions for the burst test performed by Schiemann

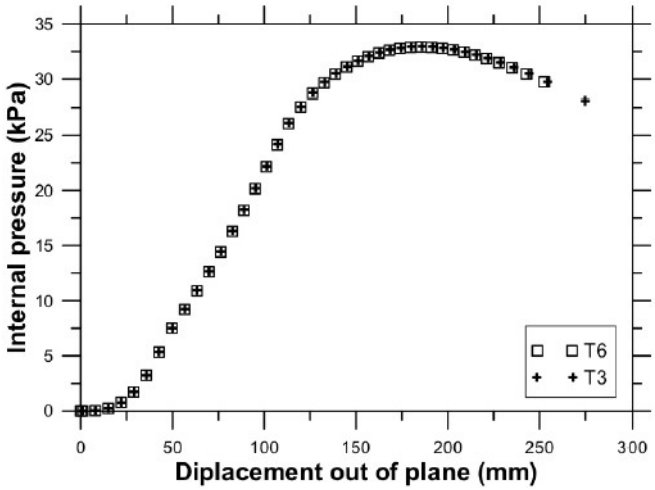

Figure 5: Pressure versus displacement results for the specimen V28 [10]; linear (T3) and quadratic (T6) triangular membrane elements.

The properties of the ETFE are extracted from the work of Schiemann [10] and are presented in table 1. A bilinear curve is used in the plastic phase due to the significant change in the hardening modulus observed experimentally.

Table 1: Material properties of specimen V28

Young's modulus (E)	417MPa
Poisson ratio (ν)	0.45
First yield stress (σ_{y_1})	14MPa
First hardening modulus (K_1)	120MPa
Second yield stress (σ_{y_2})	32MPa
Second hardening modulus (K_2)	30MPa

3.1. Results

The analysis is carried out with the cylindrical arc-length method. Table 2 presents the global convergence rate of the displacement residuum at the critical pressure for the adopted step length values (60 and 100). A small difference in the convergence is observed.

Table 2: Global convergence of the displacement residuum at the critical pressure for step length values of 60 and 100.

	step length	
	60	100
1	2.023e+01	2.166e+01
2	3.261e+00	2.850e+00
3	8.899e-02	4.937e-02
4	6.604e-05	4.682e-05
5	3.684e-09	2.359e-08

Figure 6 presents the plot of applied pressure versus the out of plane displacements for specimen V28, obtained with numerical analysis for the elastoplastic material model with large and small strains. The results obtained with the numerical model with large strains demonstrate its suitability to model this experiment. On the other hand, the numerical model with small strains is valid only in the first steps of the analysis where strains remain small. The deformed configuration of both the experimental and numerical analyses with large strains are presented in figure 7. The results are shown for two stages of the applied load, which are indicated in figure 6 with the numbers 1 (32.9kPa) and 2 (28kPa).

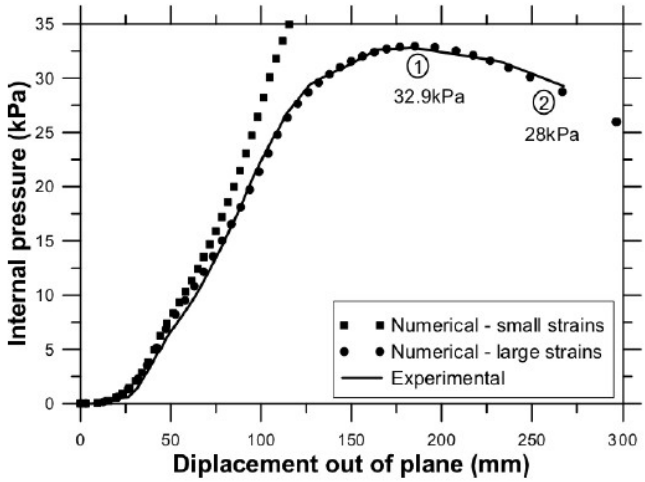

Figure 6: Pressure versus displacement results for the specimen V28 [10]; large strain, and small strain material models.

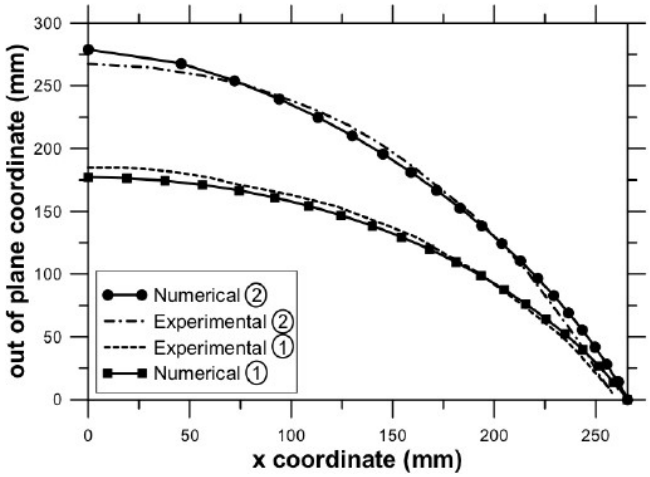

Figure 7: Deformed configuration of the specimen V28 [10] and numerical model with large strains for pressure states 1 and 2.

Figure 8 shows the stress versus strain curve in the y direction with large strains. Pressure states 1 and 2 are the same depicted in figures 6 and 7. Comparing figures 6 and 8 the non proportionality kinematics of pressure and stresses is indicated noticeable. After the critical pressure, the strains increase mightily.

Deformed configurations of the inflated circular membrane in three dimensions are shown in figure 9. The pressure states 1 and 2 are again represented.

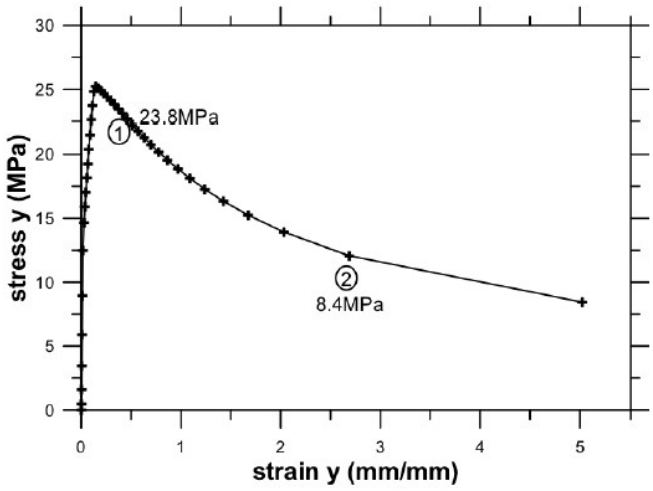

Figure 8: Stress versus strain curve in y direction

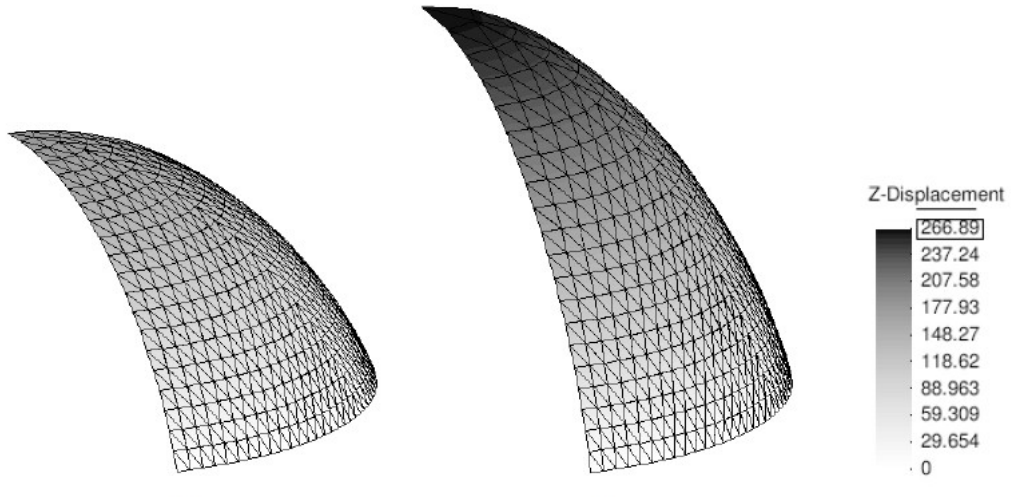

Figure 9: Deformed inflated circular membrane with the vertical displacement displacement: (a)point 1 and (b) point 2

4. Conclusion

The burst test of a circular ETFE–foil fixed at its rim is analyzed. The test is modeled with finite elements and the numerical models are compared to experimental results. The elastoplastic isotropic material model with von Mises yield criteria is considered in the numerical analysis for small and large strains. This model was adequate for the representation of plastic deformations in the ETFE.

The results obtained with the numerical analysis with large strains are in accordance with the experimental material results. On the other hand the results of the numerical analysis with small strains are valid only in the first steps of the analysis. Considering the large strain analysis in the post critical regime the amount of strains increases substantially. These results reinforce the importance of considering a material model with large strains to model this type of material.

References

[1] R. Barthel, N. Burger, and K. Saxe. Dachkonstruktionen mit ETFE-Folien. *Deutsche Bauzeitschrift*, **51**(4);72–75, 2003.

[2] Miguel Angel Caminero, Francisco Javier Montans, and Klaus-Jurgen Bathe. Modeling large strain anisotropic elasto-plasticity with logarithmic strain and stress measures. *Computers and Structures* **89**; 826- 843, 2011.

[3] Marianna A. O. Coelho. *Analysis of pneumatic structures considering nonlinear material models and pressure-volume couppling*. PhD thesis, Pontificia Universidade Catolica do Rio de Janeiro, July 2012.

[4] DuPont Fluoroproducts. *DuPont Tefzel fluorpolymer resin* - Properties Handbook.

[5] C. Galliot and R. H. Luchsinger. Uniaxial and biaxial mechanical properties of ETFE foils. *Polymer Testing*, **30**; 356–365, 2011.

[6] E. H. Lee and D. T. Liu. Finite-strain elastic-plastic theory with application to plane-wave analysis. *Journal of applied physics* , **38**; 19–27, 1967.

[7] Karsten Moritz. *ETFE-Folie als Tragelement* . PhD thesis, Technische Universitaet Muenchen, 2007.

[8] Djorkje Peric, D.R.J. Owen, and M.E. Honnor. Model for finite strain elasto-plasticity. *Computer Methods in Applied Mechanics and Engineering* , **94**; 35–61, 1992.

[9] S. Robinson-Gayle, M. Kolokotroni, A. Cripps, and S. Tanno. ETFE foil cushions in roofs and atria. *Construction and Building Materials*, **15**; 323–327, 2001.

[10] Lars Schiemann. *Tragverhalten von ETFE-Folien unter biaxialer Beanspruchung*. PhD thesis, Technische Universitaet Muenchen, 2009.

[11] J. C. Simo. Algorithms for static and dynamic multiplicative plasticity that preserve the classical return mapping schemes of the infinitesimal theory. *Computer Methods in Applied Mechanics and Engineering*, **99**; 61–112, 1992.

[12] J.C. Simo and T.J.R. Hughes. *Computational inelasticity*, volume 7. Springer Verlag, 1998.

[13] J.C. Simo and R.L. Taylor. A return mapping algorithm for plane stress elastoplasticity. *International Journal for Numerical Methods in Engineering*, **22**(3);649–670, 1986.

[14] E.A. Souza Neto, D. Peri´c, and D.R.J. Owen. *Computational methods for plasticity: theory and applications*. Wiley, 2008.

[15] R. von Mises. Mechanik der festen Koerper im plastisch-deformablen Zustand. *Nachrichten von der Gesellschaft der Wissenschaften zu Goettingen*, *Mathematisch-Physikalische Klasse*, 582–592, 1913.